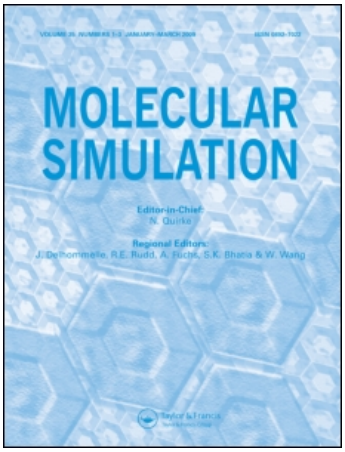

Molecular Simulation
Publication details, including instructions for authors and subscription information:
http://www.informaworld.com/smpp/title~content=t713644482

Thermal Conductivity of The Two Dimensional Soft Disk Fluid

David P. Hansen[a]; Denis J. Evans[a]
[a] Research School of Chemistry, Australian National University, Canberra, Australia

To cite this Article Hansen, David P. and Evans, Denis J.(1995) 'Thermal Conductivity of The Two Dimensional Soft Disk Fluid', Molecular Simulation, 14: 6, 409 — 416
To link to this Article: DOI: 10.1080/08927029508022034
URL: http://dx.doi.org/10.1080/08927029508022034

Molecular Simulation, 1995, Vol. 14, pp. 409–416
Reprints available directly from the publisher
Photocopying permitted by license only

THERMAL CONDUCTIVITY OF THE TWO DIMENSIONAL SOFT DISK FLUID

DAVID P. HANSEN and DENIS J. EVANS

Research School of Chemistry, Australian National University, Canberra, A.C.T. 0200, Australia

(Received October 1994, accepted November 1994)

A generalization of the Evans nonequilibrium molecular dynamics (NEMD) heat flow algorithm which suppresses the shock wave instabilities is used to calculate the thermal conductivity of the two dimensional soft disk fluid over a wide range of densities. At low densities a new transverse instability is observed at large field strengths. We see no statistically significant evidence for the presumed divergence of thermal conductivity in two dimensional systems.

KEY WORDS: Thermal conductivity, two dimensional fluid, soft disks, NEMD.

INTRODUCTION

Previously we presented a generalized version of the Evans homogeneous nonequilibrium molecular dynamics (NEMD) algorithm for simulating the flow of heat through a fluid [1]. In the original Evans algorithm [2,3] a fictitious 'heat' field is introduced into the equations of motion. This field couples to fluctuations in the fluid in such a way as to generate a heat flux. Linear response theory then shows that for small fields the ratio of the generated heat flux to the fictitious 'heat' field is identical to the average heat flux, J_q, induced by an actual temperature gradient $1/T\nabla T$. Thus the thermal conductivity of the fluid can be found by monitoring the response of the system to this fictitious 'heat' field.

This algorithm has been found to cause instabilities in two dimensional fluids when the number of particles and the fictitious heat field become sufficiently large [4]. The normal process of homogeneous heat conduction is destroyed with heat being transferred through the system via a solitary shock wave which travels at supersonic speeds and whose normal is parallel to the applied heat field. This instability was subsequently described theoretically by Mareschal and Amellal [5] and Loose [6]. The result of this instability is a sharp increase in the effective thermal conductivity of the system. As the thermal conductivity is obtained by extrapolating the flux to field ratio to zero field, this greatly reduces the efficiency with which this algorithm can be used to compute the thermal conductivity.

The generalized algorithm presented in [1] strongly inhibits the generation of this shock wave. This makes the zero field extrapolation, and hence the calculation of the thermal conductivity, much more efficient.

In the present paper we use this generalized algorithm to compute the thermal conductivity of the soft disk fluid along an isotherm from less than half the freezing density to about 50% greater than the freezing density. The scaling properties of the soft disk system mean that this single data set can be used to calculate the thermal conductivity of soft disks as a function of both temperature and density.

At low densities and high field strengths we observe a new density instability that is transverse to the induced heat field. We do not see any statistically significant evidence for the presumed divergence of thermal conductivity in two dimensions due to long time tail effects.

ALGORITHM

The details of the original Evans algorithm and our generalized algorithm are given in previous paper [1–3], hence only an overview of the new algorithm will be presented here.

From previous studies [4] it was noted that the system did not become unstable when the size of the system was small, i.e. $N \leqslant 224$. In the generalized algorithm the unit cell used in molecular dynamics simulations is divided into smaller *regions*, r, which contain a small number of particles. The force on each particle due to the heat field is then calculated from the difference between a particle's instantaneous enthalpy and the the mean enthalpy per particle of the *region* containing that particle.

The average streaming velocity of particles inside a given *region* will be non-zero. The equations of motion, the thermostat and the calculation of the thermodynamic properties within each *region* all must take this into account. The streaming velocity of each *region* can be found from,

$$\boldsymbol{u}(r_i) = \frac{\sum_{j \in r_i} \boldsymbol{p}_j}{\sum_{j \in r_i} m_j}, \tag{1}$$

where $\forall j \in r_i$ refers to all particles whose coordinates lie inside the *region* r_i, i.e. $x_{r_i} < x_i < x_{r_i} + \Delta x$ and $y_{r_i} < y_i < y_{r_i} + \Delta y$,and $\boldsymbol{p}_i$ is the peculiar momentum of particle i. The equations of motion for the generalized Evans algorithm are [1]

$$\dot{\boldsymbol{q}}_i = \frac{\boldsymbol{p}_i}{\boldsymbol{m}} \tag{2}$$

and

$$\dot{\boldsymbol{p}}_i = \boldsymbol{F}_i + \mathfrak{I}_i - \alpha(\boldsymbol{p}_i - m\mathbf{u}(r_i)), \tag{3}$$

where

$$\mathfrak{I}_i = (E_i - \hat{E}_{r_i})\boldsymbol{F}_e - \frac{1}{2}\sum_{\forall j \in r_i} \boldsymbol{F}_{ij}(\boldsymbol{q}_{ij} \cdot \boldsymbol{F}_e) + \frac{1}{2N_{r_i}} \sum_{\forall j,k \in r_i} \boldsymbol{F}_{jk}(\boldsymbol{q}_{jk} \cdot \boldsymbol{F}_e), \quad \text{where } i \in r_i. \tag{4}$$

Again $\forall j \in r_i$ refers to all particles whose coordinates lie inside the *region* r_i, i.e. r_i, i.e. $x_{r_i} < x_i < x_{r_i} + \Delta x$ and $y_{r_i} < y_i < y_{r_i} + \Delta y$, N_{r_i} is the number of particles and $\hat{E}_{r_i}$ is the mean energy of particles in *region* r_i and is calculated by summing E_i,

$$E_i = (\boldsymbol{p}_i - m\boldsymbol{u}(r_i))^2/2m + \frac{1}{2}\sum_j \Phi_{ij}, \tag{5}$$

over all particles in that region.

In (3), α is the thermostat multiplier. A thermostat must be incorporated into the equations of motion in order to remove the heat produced in the system by the external field. Since the peculiar velocity of each particle will depend on which *region* a particle is in, we use the Nose-Hoover thermostat [7,8] which uses an integral feedback mechanism. The thermostat multiplier, α, is calculated from the time integral of the difference between the kinetic temperature, T, and the desired temperature of the system T_0, i.e.

$$\dot{\alpha} = \frac{T - T_0}{Q}, \tag{6}$$

where for a two dimensional fluid the kinetic temperature $T$is given as

$$T = \frac{1}{Nk_B}\sum_r \sum_{i \in r} \frac{(\boldsymbol{p}_i - m\boldsymbol{u}(r_i))^2}{2m}. \tag{7}$$

Q is an arbitrary intensive constant which governs the feedback rate. The heat flux vector can be calculated by

$$\boldsymbol{J}_Q A = \sum_{i=1}^{N} \frac{(\boldsymbol{P}_i - m\boldsymbol{u}(r_i))E_i}{m} - \frac{1}{2}\sum_{i,j=1}^{N} \frac{\boldsymbol{q}_{ij}(\boldsymbol{p}_i - m\boldsymbol{u}(r_i))\cdot \boldsymbol{F}_{ij}}{m}, \tag{8}$$

where the system area, A, is related to the number of particles, N, and the density, ρ, by $\rho = N/A$. The thermal conductivity coefficient can then be found from the ratio of the heat flux vector to the applied heat field,

$$\lim_{F_e \to 0} \boldsymbol{J}_Q = \lambda T \boldsymbol{F}_e. \tag{9}$$

The heat field $\boldsymbol{F}_e$ was chosen to be parallel to the x-axis. In Ref. [1], numerical results using *regions* of two different geometries were considered: column shaped *panels*, where the simulation box is subdivided into strips of area $\Delta x.L$, where L is the width of the entire simulation cell, and rectangular shaped *plackets*, where the simulation box is subdivided into rectangular regions of area $\Delta x.\Delta y$. When the system was divided into *panels*, the instability was greatly reduced and at small applied fields appeared to vanish completely. However, at larger fields some instability seemed to remain, the microstructure of these systems revealing two shock waves at 45° to the applied field and 90° to one another. When the system was divided into *plackets* these shock waves completely vanished, with the microstructure of the system being quite homogenous in both density and heat.

THE SOFT DISK THERMAL CONDUCTIVITY

The simulations were carried out on two dimensional systems of $N = 3584$ particles at the same temperature ($T = 1$) as in our previous paper. (All variables are in reduced units, being reduced by the potential parameters σ and ε and the mass, m). Again the soft disk potential $\Phi(r) = \varepsilon(\sigma/r)^{12}$ was used, with a cutoff, $r_c = 1.5$. The heat field $\boldsymbol{F}_e$, was again chosen to be parallel to the x-axis, $\boldsymbol{F}_e = i\boldsymbol{F}_{ex}$. The equations of motion were solved using the Gear fifth order algorithm with reduced timesteps between 0.002 and 0.004. The simulations were carried out on a Fujitsu AP1000 using a spatial decomposition algorithm [9]. The heat flux vector was evaluating using (8), from runs of between 200 000 and 500 000 timesteps after the system reached a steady state. The thermal conductivity was calculated for three different applied heat fields, $F_{ex} = 0.01, 0.05$, and 0.1. The effective conductivity could then be calculated from Equation 9.

The calculations were performed using two different sized *plackets*.

Case (A) $\Delta x = \dfrac{\sqrt{N/\rho}}{10}$ and $\Delta y = \dfrac{\sqrt{N/\rho}}{4}$, to make a total of 40 *plackets* and

Case (B) $\Delta x = \dfrac{\sqrt{N/\rho}}{8}$ and $\Delta y = \dfrac{\sqrt{N/\rho}}{8}$, to make a total of 64 *plackets*. Case (A) was the same used in Ref. [1].

Figure 1 (a) and (b) show the thermal conductivities at different external field strengths for two different densities, $\rho = 0.8$ and $\rho = 1.1$ respectively. Within statistical uncertainties the extrapolated conductivities are independent of the number of *plackets*. However, at higher fields the nonlinear thermal conductivity (which has no thermophysical meaning) is dependent on the number of *plackets*. For case (A) it is reasonable to fit a polynomial to the points, while for case (B) a linear extrapolation to zero field can be made. However, to be consistent, the thermal conductivity for each of the two *placket* sizes is calculated by making a linear extrapolation to zero field for the smaller fields, i.e. $F_{ex} = 0.01$ and 0.05, and then including the larger field, $F_{ex} = 0.1$, and making a parabolic extrapolation to zero field. This process allows an estimate of the error to be made, as can be seen in Figures 1 (a) and (b).

Table 1 shows the thermal conductivities, calculated in the way just described, for the two different *placket* sizes, cases (A) and (B), at different densities. For $\rho = 0.4$ and 0.5 the conductivities are calculated using only $F_{ex} = 0.01$ and 0.05 due to instabilities which are discussed in the next section.

Figure 2 shows the two dimensional thermal conductivity along the $T = 1$ isotherm, from the data in Table 1. The soft disk melting and freezing points are shown on the isotherm as arrows at $\rho = 0.986$ (freezing point) and $\rho = 1.0066$ (melting point) [10]. The thermal conductivity of the soft disk fluid increases gradually between $\rho = 0.6$ and $\rho = 1.0$, however after $\rho = 1.0$ the thermal conductivity of the fluid rises quite rapidly. This is consistent with the melting and freezing points. In the solid region of the phase diagram, the particles are much close together and conduction is by phonons, which is different to the heat conduction mechanism in a liquid.

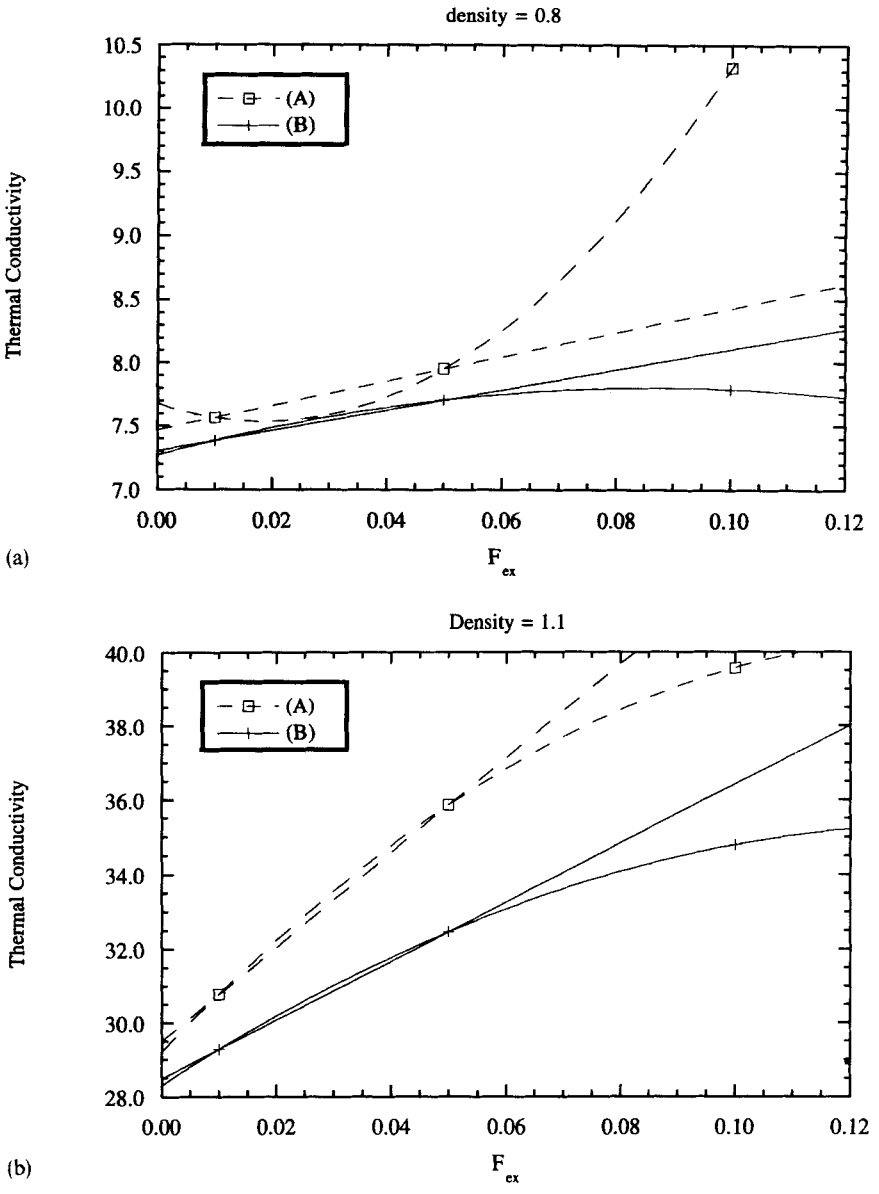

Figure 1(a) and (b) The thermal conductivities at different field strengths. The thermal conductivity for each of the two *placket* sizes, case (A) and (B) is calculated by making a linear extrapolation to zero field for the smaller fields, i.e. F_e 0.01 and 0.05, and then including the higher field, $F_s = 0.01$, and 0.05 making a parabolic extrapolation to zero field.

NEW INSTABILITIES

At densities lower than $\rho = 0.6$ the thermal conductivity is quite easily calculated for the smaller fields. However at $F_{ex} = 0.1$ the system failed to maintain a steady state. Upon

Table 1 The Thermal Conductivities for the Two Different *Placket* Sizes, Cases (A) and (B).

Density	*Conductivity (A)*	*Conductivity (B)*
0.40	2.2 ± 0.2	
0.50	2.9 ± 0.2	
0.60	4.1 ± 0.1	4.07 ± 0.03
0.70	5.7 ± 0.2	5.03 ± 0.01
0.80	7.6 ± 0.2	7.29 ± 0.04
0.90	10.0 ± 0.1	10.03 ± 0.05
0.9238	11.8 ± 0.2	11.71 ± 0.05
0.975	11.7 ± 0.9	13.2 ± 0.5
1.00	15.5 ± 0.3	14.82 ± 0.01
1.025	20.5 ± 0.5	19.1 ± 0.1
1.10	29.4 ± 0.3	28.4 ± 0.2
1.20	51.4 ± 2.6	51.4 ± 0.5

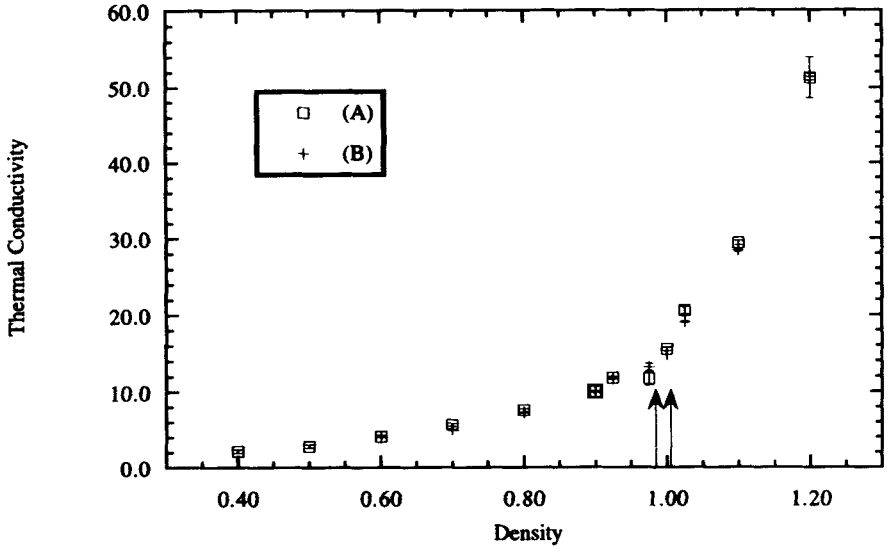

Figure 2 The two dimensional soft disk thermal conductivity. The soft disk melting and freezing points are shown as arrows at $\rho = 0.986$ (freezing point) and $\rho = 1.0066$ (melting point).

investigation of this phenomenon, a new instability was found. Figure 3 shows the grey scale image of a system of 3584 particles, using the new generalized algorithm, and with a field strength of $F_{ex} = 0.1$ and density, $\rho = 0.3$. Each disk represents the position of a particle within the simulation cell. The disks are colored in proportion to their excess enthalpy's compared to the mean enthaply per particle of the system (darker particles have greater enthaply). The system seems to be divided into two fluids with different densities- a dense fluid and a more sparsely populated fluid.

Superficially this image (Figure 3) looks like the shock wave instability discussed in previous papers [1,4]. However it differs in three very significant ways. Firstly the

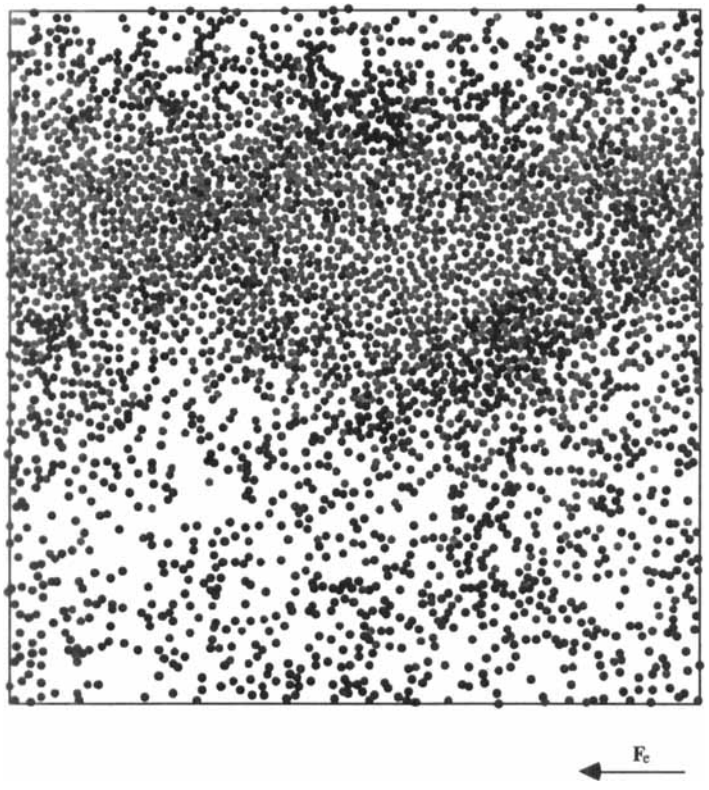

Figure 3 The grey scale image of a 3584 particles, using the new generalized algorithm with 8 × 8 *regions*, and with a field strength of $F_e = 0.1$. Each disk represents the position of a particle within the simulation cell. Each disk is colored in porportion to it's excess enthaply compared to the mean enthaply per particle of the system (darker particles have greater enthaply). The system seems to be divided into two fluids with different densities a dense fluid and a more sparsely populated fluid.

normals to the isochors and the isoenthalps are perpendicular to the heat field. (In the shock wave instability the normals are parallel to the field.) Secondly, the spatial inhomogeneities in Figure 3 are stationary, rather than travelling as in the shock wave instability. Finally, the inhomogeneities in the fluid continue to increase over time. Thus the system never reaches a steady state, and the program becomes unable to continue calculating the time evolution of the system.

CONCLUSION

In this short note a generalization of the Evans thermal conductivity algorithm has been used to calculate the two dimensional soft disk thermal conductivity.

The generalized algorithm suppresses the shock wave instability observed in the Evans algorithm, vastly increasing the efficiency of the zero field extrapolation, required by NEMD to calculate the Navier-Stokes thermal conductivity. This allows the thermal conductivity at various densities to be calculated.

However, at low densities another instability, this time characterized by the density of the fluid, is found. It seems as though the number of *plackets* which the system is divided into is again important for the time taken for this instability to form and for the system to fail to maintain a steady state.

The most likely way to remove both the instabilities is to divide the system into smaller *plackets*. A genuinely local based algorithm, where the heat field couples to fluctuations in the particle enthaply of the nearby neighbors of each particle, instead of fluctuations in the *region* which each particle is in, seems to offer the best hope of minimizing the occurrence of all instabilities. However, the algorithm which has been used in this paper to calculate the thermal conductivity algorithm has proved sufficient for calculating the thermal conductivity over a wide range of densities.

We have thus produced the first set data set from which one can extract the thermal conductivity of a two dimensional system as a function of both temperature and density. In reference [1] we showed that two dimensional thermal conductivity obtained using this algorithm shows an insignificant number dependence (at least for $T= 1, \rho = 0.9238$ and N ranging between 56 and 3548) and that the results agree, within estimated statistical uncertainties, with the less efficient Green-Kubo technique.

We see no evidence for the presumed divergence of Navier-Stokes transport coefficients in two dimensional systems [11]. In this respect the two dimensional soft disk data are analogous to the corresponding two dimensional viscosity data [12]. It may be that the processes thought to be responsible for the divergence all Navier-Stokes transport coefficients in two dimensional systems are 'hidden' as we have previously argued for shear viscosity. It is hoped that the present data may stimulate further work to better understand this matter.

References

[1] D. P. Hansen and D. J. Evans, "A generalised heat flow algorithm", *Mol. Phys.*, **81**, 767 (1994)
[2] D. J. Evans, "Homogeneous NEMD Algorithm for Thermal Conductivity: Application of Non-Canonical Linear Response Theory", *Phys. Lett.*, **91A**, 457 (1982)
[3] D. J. Evans and G. P. Morriss., *Statistical Mechanics of Nonequilibrium Liquids*, (Academic Press, 1990).
[4] D. J. Evans and H J. M. Hanley, "Heat Induced Instability in a Model Liquid", *Mol. Phys.*, **68**, 97 (1989).
[5] M. Mareschal and A. Amellal, "Thermal Conductivity in a One Dimensional Lennard Jones Chain by Molecular Dynamics", *Phys. Rev. A*, **37**, 2189 (1988).
[6] W. Loose, "Thermal Transport in Gases via Homogeneous Nonequilibrium Molecular Dynamics", *Phys. Rev. A*, **40**, 2625 (1989).
[7] S. Nose, "A Molecular Dynamics method for Simulations in the Canonical Ensemble" *Mol. Phys.*, **52**, 255 (1984).
[8] W. G. Hoover, "Canonical Dynamics-Equilibrium Phase Space Distributions", *Phys. Rev. A*, **31**, 1695 (1985).
[9] D. P. Hansen and D. J. Evans, "A Parallel Algorithm for Nonequilibrium Molecular Dynamics Simulation of Shear Flow on Distributed Memory Machines", *Mol. Sim.*, (to appear).
[10] D. J. Evans, "Melting in Soft Disk Systems", *Phys. Lett.*, **88A**, 48 (1982).
[11] P. Resibois and M. de Leener, *Classical Kinetic Theory of Fluids*, (Wiley, 1977) and references therein.
[12] D. J. Evans and G. P. Morriss, "Shear Thickening and Turbulence in Simple Fluids" *Phys. Rev. Lett.*, **56**, 2172 (1986) and G. P. Morriss and D. J. Evans, "Nonlinear Shear Viscosity in Two Dimensions", *Phys. Rev.*, **39**, 6335 (1989).